Physics of Plasmas

Target heating in femtosecond laser–plasma interactions: Quantitative analysis of experimental data

Cite as: Phys. Plasmas **28**, 023101 (2021); https://doi.org/10.1063/5.0035356
Submitted: 28 October 2020 . Accepted: 11 January 2021 . Published Online: 01 February 2021

Eran Nardi, Zeev Zinamon, Evgeny Stambulchik, Ulf Zastrau, Eyal Kroupp, Ingo Uschmann, Gerhard G. Paulus, and Yitzhak Maron

View Online Export Citation CrossMark

AIP Advances
Fluids and Plasmas Collection
READ NOW

AIP Publishing

© 2021 Author(s).

Physics of Plasmas ARTICLE scitation.org/journal/php

Target heating in femtosecond laser–plasma interactions: Quantitative analysis of experimental data

Cite as: Phys. Plasmas **28**, 023101 (2021); doi: 10.1063/5.0035356
Submitted: 28 October 2020 · Accepted: 11 January 2021 ·
Published Online: 1 February 2021

View Online Export Citation CrossMark

Eran Nardi,[1,a)] Zeev Zinamon,[1] Evgeny Stambulchik,[1] Ulf Zastrau,[2] Eyal Kroupp,[1] Ingo Uschmann,[3] Gerhard G. Paulus,[3] and Yitzhak Maron[1]

AFFILIATIONS

[1]Faculty of Physics, Weizmann Institute of Science, Rehovot 7610001, Israel
[2]European XFEL GmbH, 22869 Schenefeld, Germany
[3]Institut für Optik und Quantenelektronik, Friedrich-Schiller-Universität Jena, Max-Wien-Platz 1, D-07743 Jena, Germany

[a)]**Author to whom correspondence should be addressed:** eran.nardi@weizmann.ac.il

ABSTRACT

We study electron heating and stopping power in warm dense matter as formed in interactions of sub-picosecond high-intensity lasers with solid bulk targets. In such interactions, an intense beam of forward moving relativistic electrons is created, inducing a compensating return current and generating characteristic $K\alpha$ x-ray radiation along the propagation path. The theoretical calculations presented here are inspired by, and tested against, a previously published study that provides bulk-temperature and absolutely calibrated $K\alpha$ radial profiles. By using Monte Carlo simulations, the experimental data allow for inferring the flux of the relativistic electrons, which is a crucial input for the target heating calculations. For the latter, a "rigid beam" model is employed, describing the central, nearly homogeneous, part of the target. The comparison with the experiment shows a fairly good agreement. For the conditions analyzed, we find that the effect of the return current is dominant both in the target heating and in the beam stopping.

Published under license by AIP Publishing. https://doi.org/10.1063/5.0035356

I. INTRODUCTION

Ultra-short powerful lasers, focused onto the surface of a solid target, generate intense beams of forward moving relativistic electrons, much in excess of the Alfvén current.[1] The study of the interaction of these electrons with various targets is an area of intense research, both in experiment and in theory. The interest in this field stems from its important applications, such as the fast ignitor approach to inertial confinement fusion,[2] the generation of intense ultra-short $K\alpha$ pulses, ion acceleration,[3] and the production and study of warm dense matter (WDM).[3,4] The latter is an exotic state of matter characterized by a significant Coulomb coupling and pronounced quantum effects. In other words, the thermal energy of the bulk WDM electrons is comparable to the typical inter-particle Coulomb potential and/or the Fermi energy.[5] Evidently, the electron temperature is an important subject in the studies of WDM, with those providing quantitative comparison of theoretical and experimental results being of particular interest. To name a few, Martinolli *et al.*[6] observed spectrally shifted Al $K\alpha$ lines and drew conclusions regarding the temperature, modeling target heating by means of a hybrid transport code; Santos *et al.*[7,8] also measured target temperature while calculating target heating by means of a hybrid code and by a semi-analytical model; Honrubia, Antonicci, and Moreno[9] also studied temperatures obtained in Al foils by means of a hybrid code; Passoni *et al.*[10] dealt with a semi-analytical model for the heating of Al foils and obtained bulk electron temperatures on the order of 100 eV (but did not compare these calculations with experimental data). An additional work on this topic is given by Perez *et al.*[11] and Soloviev *et al.*[12]

This paper deals with the theoretical evaluation of electron-beam heating in a thick titanium target. We suggest a physically sound model that involves virtually no free parameters. The calculated results are compared with the experimental ones, while the input data for the calculations are taken from the same experiment. The experimental data which this paper addresses are the radial electron-temperature and absolutely calibrated $K\alpha$-intensity profiles.[13,14] Some of the ideas presented here were discussed by some of us in a previous publication.[15] A related paper, focusing on electron refluxing and electric-field intensity outside the foil, is under preparation.[16]

In Sec. II, we describe the experimental data upon which our calculations are based. In Sec. III, we deal with target heating, where as a

Published under license by AIP Publishing

first step, we make use of the experimental $K\alpha$ data to obtain the absolute electron beam intensity. Care is given in obtaining the two major physical quantities needed for an accurate simulation of target heating, the specific heat, and the resistivity of the Ti plasma electron subsystem. We then calculate beam heating dealing with direct and return-current heating and present the results in Sec. IV. Beam stopping is also calculated, highlighting the effect of the return-current heating on the stopping.[7,8,17–19]

II. EXPERIMENTAL DATA USED

The theoretical analysis presented in this paper makes use of the data obtained from the experiment on ultra-intense femtosecond laser interactions with Ti targets.[13] For convenience, a sketch of the experimental setup is given in Fig. 1. Here, a 14-J, 330-fs laser beam nearly normal to the target surface is focused to a spot of 8 μm diameter (FWHM), reaching an intensity of about 5×10^{19} W/cm^2.

The temperature analysis of this experiment was based on a detailed line shape modeling of Ti spectra.[20] For the present study, a subset of the results obtained using the bulk target, irradiated by the laser operating at the fundamental frequency, is used. We point out that a constant factor was erroneously introduced in the $K\alpha$-yield data presented in Fig. 4 of the original study[13] (not affecting any of the conclusions there). The relevant radial distributions of the bulk electron temperature and the corrected $K\alpha$ flux are given in Fig. 2. The total time-integrated number of $K\alpha$ photons emitted in 4π steradians is determined to be 3.4×10^{11}.

We define the z axis as the axis of symmetry of the target with the peak laser intensity impinging at $z = 0$. It is important to note that the experimental data are time- and z-integrated.

III. DESCRIPTION OF THE MODEL

A. Basic assumptions

As seen from Fig. 2, the target comprises a stronger heated, bright core and a much colder weakly radiating halo. The focus of the present study is the target core, which is approximated by a homogeneously heated 30-μm-radius cylinder. An important point is the assumption that the heat flow from this volume is negligible during the laser pulse.

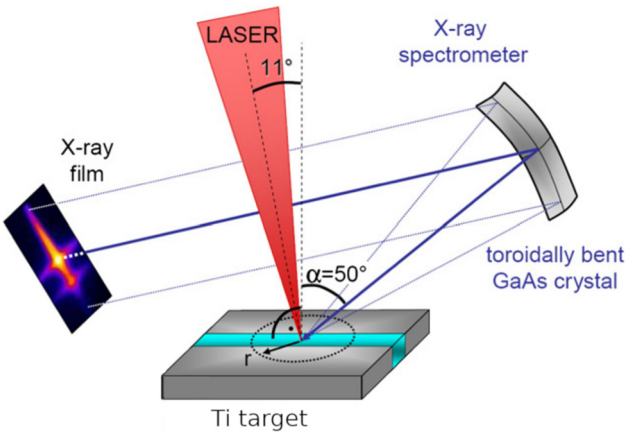

FIG. 1. Schematic of the experimental setup. Reproduced with permission from Zastrau *et al.*, Phys. Rev. E. **81**, 026406 (2010).[13] Copyright 2010 American Physical Society.

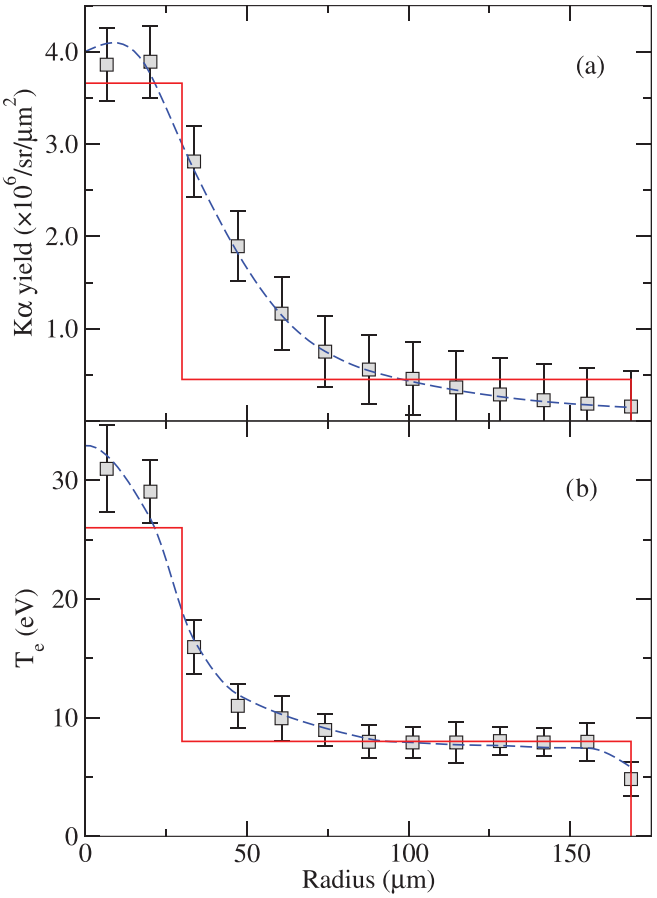

FIG. 2. Experimental data. (Adapted from Ref. 13.) Radial distributions of the integrated $K\alpha$ yield (a) and the bulk electron temperature (b). The solid lines correspond to a step-like model approximation separating the homogeneously heated bright target core from the colder halo.

Indeed, in a previous study,[15] the heat-conduction times on the order of microseconds were inferred, significantly longer than the laser-pulse duration. The same conclusion was reached by investigating the time development of the propagation of heat from an instantaneous cylindrical source. It was also noted in that study that the great similarity of the temperature distribution in the transverse direction to that of the $K\alpha$ distribution[13] testifies to the conclusion that the lateral heat diffusion is small. Heat loss from the front of the target can also be neglected.[10]

By investigating the bulk target, the complicating effects associated with refluxing do not have to be accounted for. Furthermore, we ignore the region of the lower-density plasma formed at the front of the target, where temperatures on the order of keV have been measured.[6] Eidmann *et al.*[21] also measured temperatures of about 800 eV at shallow depths up to 400 nm. The heat in the front-surface layers will take much time, at least on the order of 10s of ps, to diffuse into the bulk as a result of a relatively low value of the thermal conduction.[10] Again, we are in effect assuming here that the temperature is being measured for the extent of the time when the $K\alpha$-producing electron beam is on, which does not extend much beyond the 330-fs laser pulse.

Published under license by AIP Publishing

In the present analysis, we view the laser as a source for producing an intense electron beam assumed to be constant in time during the laser pulse (evidently, after averaging over a few periods of the laser-field oscillations). Although this is, in general, not true (e.g., see Ref. 22), detailed knowledge of the temporal electron-beam shape is of minor relevance given the time-integrated nature of the experimental data, not affecting the principal conclusions drawn here.

Another assumption in the modeling is that the energetic electrons are normally incident on the target and the beam density is fixed throughout, with no scattering and neglecting electromagnetic fields. This is in effect the rigid beam approximation.[23,24] The simplified rigid beam model has also been used in other studies (e.g., see Refs. 10 and 25).

In support of the perpendicular beam interaction assumption, we cite diverging-beam studies. The "ballistic" nature of the forward moving fast electron beam was reported by Green *et al.*,[26] giving for the experimental conditions analyzed here a diverging angle of about 30°. An effective diverging angle of 24° at $4 \times 10^{19}\,\mathrm{W/cm^2}$ was measured,[27] and a recent analysis of bremsstrahlung data yields an incident electron angular spread of $15 \pm 8°$ at $2 \times 10^{19}\,\mathrm{W/cm^2}$.[28] The relatively small divergence of the fast electron beam is probably in part due to magnetic collimation,[29] which could also be the case here. The result of this is an advancing beam not too different from the parallel beam assumed in the present modeling. Our approach, which makes the problem amenable to a straightforward modeling, is different from more elaborate studies employing particle-in-cell simulations, e.g., see Refs. 6, 9, and 30.

B. Beam heating of the target

Numerous publications have dealt with the response of the target to the ultra-intense electron currents far in excess of the Alfvén limit.[29,31,32] Electrons can propagate because of the return current, which is assumed to be equal in magnitude to that of the incoming beam. The background target electrons are put into motion as a result of the electric fields set up by the fast electrons. The time of charge neutralization is estimated to be $\lesssim$1 fs.[17]

Both the direct and return currents heat the target. The temperature increase dT_e of the electronic subsystem due to the deposited beam energy dE, which is transferred to the bulk target electrons, is obtained from

$$dE = n_a C_e dT_e, \tag{1}$$

where n_a is the atomic density and C_e is the per-atom specific heat of the electronic component of the target. The thermal coupling of the electron subsystem to the ion subsystem within the 330-fs pulse duration is neglected due to the substantially longer times characteristic of this process.[21]

The direct, or collisional, beam-energy deposition is given by

$$P_{\mathrm{col}} = Sj/e, \tag{2}$$

where $S = -dE/dx$ is the stopping power, j is the current density, and e is the elementary charge. The return current resistively heats the background electron plasma, contributing

$$P_{\mathrm{res}} = \eta j^2, \tag{3}$$

where η is the target resistivity. Finally, the evolution of the target electron temperature is governed by

$$n_a C_e \frac{dT_e}{dt} = Sj/e + \eta j^2. \tag{4}$$

C. Absolute electron flux

We determine the absolute electron beam intensity incident on the bulk using Monte Carlo (MC) simulations. These simulations provide the number of fast electrons required to produce one detectable $K\alpha$ photon. The total number of electrons N_{fast} hitting the target is then obtained by multiplying this value by the experimentally determined time-integrated number of $K\alpha$ photons emitted in 4π radians from the 30-μm-radius target core (Fig. 2). Finally, N_{fast}, divided by the laser-pulse duration and the core front-surface area, gives the fast-electron flux.

As outlined in Sec. III A, our approach is based on the rigid beam approximation with the electron beam incident normally on the target. However, since the target heating crucially depends on the current density, see Eq. (4), here we use a more realistic model in order to increase the accuracy in inferring j. Specifically, we impose a 30° angular distribution of the electron beam, as suggested in Ref. 26 for the relevant experimental conditions (see Sec. III A). The electron energy spectrum is assumed to have a Boltzmannian $\exp(-E/T_{\mathrm{fast}})$ tail with T_{fast} set at 1 MeV. This value is between the ponderomotive and Beg values for the conditions of the present experiment and agrees with the Beg-inspired fit of Lefebvre *et al.*[33]

The electron motion within the target is treated in detail, accounting for scattering by means of the Bethe–Molière formalism[34] as well as for electron slowing down.[35] At every time step in the simulation, the $K\alpha$ emission probability is calculated on the basis of the K-shell hole production cross section σ_K. This is multiplied by the probability that the photon is on its way to the detector, as positioned in the experiment,[13] and escapes the target, also accounting for the absorption; the mean free path of $K\alpha$ in the Ti target is about 20 μm.[36]

We use σ_K as given by Llovet *et al.*[37] with the appropriate fluorescence yield.[38] To the best of our knowledge, there are no experimental data on the cross section for the K-shell hole production in the relevant region for titanium, but for vanadium, the next species in the periodic table, the experimental point at 2 MeV agrees well with the theory. On the other hand, we note that for Ti at the lower 100 keV energy (not directly relevant to the present research), the experimental result is significantly lower than the theoretical value.[37]

Within the MC framework, the return current and the associated resistive stopping cannot be accounted for in an *ab initio* way. On the other hand, as will be shown in Sec. IV B, the resistive stopping is more efficient than the collisional one. In order to approximately account for it, we performed another simulation where it was assumed that the collisional energy loss is larger by a factor of four.

The results of the two simulations are presented in Table I, showing the number of incident fast electrons required to produce one detectable $K\alpha$ photon and the current density. For the enhanced stopping assumption, more electrons are needed to produce a $K\alpha$ compared to the conventional stopping. In the former case, the larger stopping power shortens the electron penetration depth, and as a result, more backscattering events occur here. The backscattered electrons neither produce $K\alpha$ in the vacuum region nor return to the target.

Published under license by AIP Publishing

TABLE I. Results of the MC simulations, assuming regular and enhanced stopping models (see the text). The number of incident electrons needed to produce a single detectable $K\alpha$ photon $N_{K\alpha}$ and the fast-electron current density j are shown.

Collisional stopping	$N_{K\alpha}$	j (A/cm^2)
Regular	95	1.8×10^{11}
Enhanced	123	2.3×10^{11}

We note that the efficiency of the energy transferred to the fast electrons ϵ_L, defined as a ratio of the total energy of the fast electrons to the energy of the laser beam, is around 0.5 in both cases. This value is in agreement with other studies finding $0.1 < \epsilon_L < 0.9$.[2] We also note that the current density inferred corresponds to the fast-electrons density of about 4×10^{19} cm^{-3}, i.e., on the order of 10^{-4} of the density of the bulk electrons.

D. Physical data

In Eq. (4), C_e and η are functions of T_e, while $n_a = 5.65 \times 10^{22}$ cm^{-3} is constant, i.e., neglecting any hydrodynamic expansion of the bulk target during the short laser pulse.[39] S is also assumed to be constant, equal to the stopping power of the cold titanium, 6.0 MeV/cm,[40] since for the relatively low bulk temperatures attained here, the plasma effects on the stopping can be neglected.[35]

$C_e(T)$, which is an important quantity in the present modeling, is obtained from the average-atom model by Liberman.[41] The basis here is the calculation of the total electronic energy content of the Wigner–Seitz atomic system, which includes the energy associated with the bound electrons, free electrons (employing the Fermi–Dirac statistics), and the resonance or band electrons, as a function of temperature. The derivative of the calculated electronic energy with respect to the temperature gives $C_e(T)$. In Fig. 3, we present the specific heat per atom in units of the Boltzmann constant k_B as a function of temperature. We observe a rapid rise followed by flattening out.

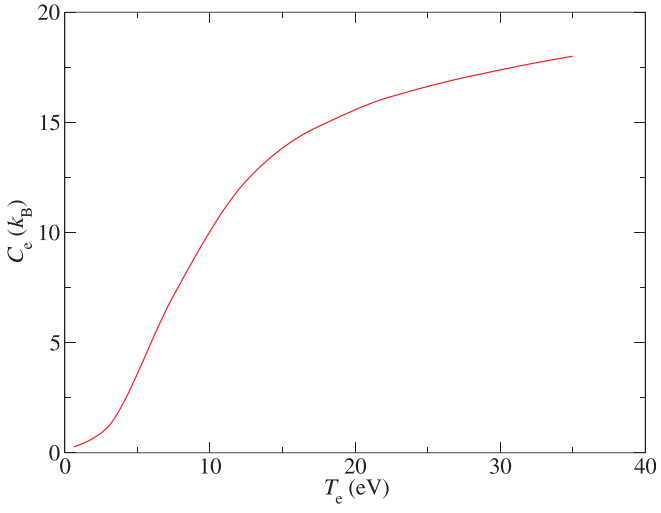

FIG. 3. Specific heat of Ti per atom as a function of temperature at the solid-state density.

This is qualitatively similar to the dependence of C_e on the temperature as suggested in Ref. 10. There, it is assumed that $C_e = 3/2 k_B N_f$ in the flat region above the Fermi energy, which would give less than half of what we obtain at 30 eV. Here, N_f is the number of free electrons per atom as given by the average-atom model. A detailed discussion on the complexity of calculations of C_e at the lower temperatures is discussed in the literature[42] in connection with electron phonon coupling and will not affect our basic conclusions.

In our determination of the resistivity, we are guided by the experiment of Sandhu, Dharmadhikari, and Kumar,[43] who measured the electron collision frequency ν_e (an effective frequency of electron–electron collisions governing energy transfer) of Cu in a femtosecond laser interaction experiment, similar to the experiment analyzed here. The resistivity was calculated using the Drude model as

$$\eta = \frac{m_e \nu_e}{e^2 n_f}, \tag{5}$$

where $n_f = n_a N_f$ is the free-electron density. As can be seen from Fig. 3 of Ref. 43, there are three qualitatively different regimes: low-T, middle-T, and high-T. The collision frequency in the middle-T (between ∼10 and ∼30 eV) region essentially attains collisional saturation,[44] given by $\nu_e^{\max} = v_e/r_0$, where v_e is the electron thermal velocity and r_0 the inter-atomic distance. This implies that an electron freely travels at least the inter-atomic distance between scattering events.[43,45] It is assumed that in this region (which contributes most of the heating), the resistivity of the titanium WDM also attains the collisional saturation. Milchberg *et al.*,[45] who measured the Al resistivity in a femtosecond laser experiment, also found "resistivity saturation" in the analysis of their data. Collisional saturation, which results in resistive saturation, is assumed in Ref. 10 as well as by Eidmann *et al.*[46] in their schematic representation of resistivity while analyzing sub-picosecond laser–plasma experiments. A recent study of Faussurier and Blancard[47] also obtains resistivity saturation in Al in the WDM regime employing the average-atom Ziman–Evans approach. A very recent study by Wetta and Pain,[48] also using the Ziman–Evans approach, gives, too, a flattening out of the Al conductivity in the temperature range between about 20 and 40 eV. In Table II, we give the values of N_f and the calculated values of the resistivity, in the collisional saturation region. We note that although N_f increases with temperature, the resistivity does not decrease, remaining almost constant. This is because $\nu_e^{\max}$ also increases since the electron thermal velocity v_e increases with temperature.

The resistivity in the low-temperature region, leading up to the resistivity saturated regime, was experimentally shown in Cu[43] to be determined by the electron–electron interaction, which scales as $\propto T_e^2/E_F$, where E_F is the Fermi energy. This is reasonable in view of

TABLE II. Saturated resistivity η and the number of free electrons per atom in Ti, N_f, for different temperatures.

T_e (eV)	N_f	η ($\mu\Omega \cdot$ cm)
15	3.23	189
20	3.76	187
25	4.25	185
30	4.69	184

Published under license by AIP Publishing

the fact that the ions remain much colder than the electrons due to the relatively long electron–ion relaxation time. Hence, the electron–phonon scattering is less pronounced than the electron–electron collisions as the temperature of the electrons increases. In our approach, we obtain the resistivity for Ti in this low-temperature region by scaling the Cu resistivity values[43] by the ratio of the saturated resistivity of Ti to that of Cu at 20 eV. Such a scaling is justified by the rather close values of E_F of both metals, 7.1 eV (Ref. 49) and 8.8 eV (Ref. 50) for Cu and Ti, respectively.

Similarly, for the high-temperature, $\propto T_e^{-3/2}$ Spitzer regime, we assume that in Ti, the onset of this regime is at the same temperature as in Cu. Reference 10 suggests that the inflection point to the Spitzer regime occurs at about $10E_F$, whereas experimentally, it was found to be about $5E_F$.[43] On the other hand, in Al, where the Fermi energy is 11.3 eV,[49] the experimentally determined saturated resistivity and the onset of the Spitzer regime are at significantly higher temperatures than for Cu: the Spitzer regime starts at ∼40 eV for Cu vs ∼90 eV for Al.[45]

Following these considerations, the transition to the Spitzer resistivity in Ti was assumed to be at $5E_F$ as in Cu. The resulting resistivity as a function of T_e is shown in Fig. 4.

An interesting resistivity calculation was presented for Si in a laser–plasma electron transport experiment by Maclellan *et al.*[51] These authors calculate resistivity by means of the Lee–More model,[52] also with the quantum molecular dynamics calculation and by the Spitzer model. Their results are similar in shape and magnitude to our Ti resistivity.

IV. RESULTS

We are now ready to solve Eq. (4) numerically. The calculations start with $T_e = 0$ at $t = 0$ and terminate at the end of the incident fast electron pulse, assumed to coincide with the laser-pulse duration, as discussed in Sec. III A. The calculations were performed for two values of the electron flux (see Sec. III C) to provide an estimate of uncertainties in our modeling.

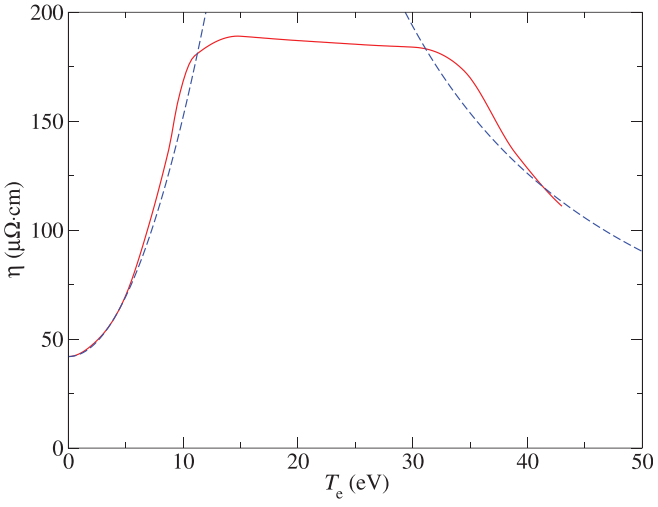

FIG. 4. The electrical DC resistivity of Ti as a function of the electron temperature. The dashed lines show the low- and high-temperature model scalings, with a collisional-saturation regime clearly seen in between. The scalings are due to the electron collision frequency (thus ignoring the variation of the free-electron density n_f).

A. Target temperature

In Fig. 5(a) given is the bulk temperature as a function of the pulse duration time. As can be seen from the figure, the final temperature, calculated with the inclusion of both the direct and resistive heating, is in rather good agreement with the experimentally determined ones for the inner 30-μm of the bulk target, of 30–35 eV.[13,14]

We remind that the measurements were time-integrated. However, it is plausible that the experimentally inferred temperatures are closer to the final values (reached by the end of the laser pulse) than to the arithmetically averaged ones. Indeed, the temperature measurements were based on the $K\alpha$ shapes, and therefore, one should consider a *weighted* average with the weighting function given by the $K\alpha$ intensity, which is roughly proportional to the fast-electron current. On the other hand, the latter was shown[22] to increase with time, with a pronounced peak around the laser-pulse end.

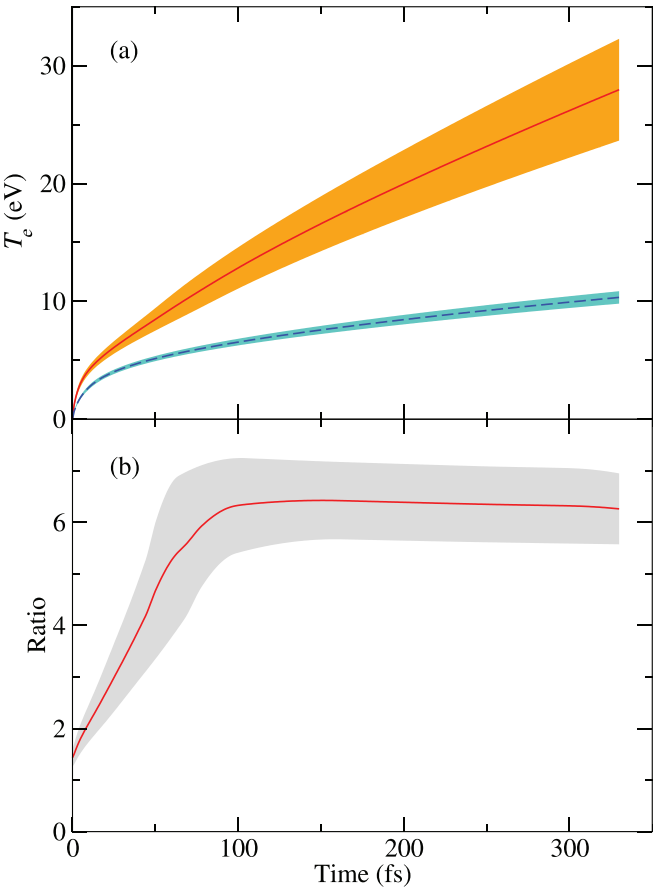

FIG. 5. Results of the calculations. (a) The target temperature. Solid curve: full calculations; dashed curve: only direct collisional heating retained. (b) The ratio of resistive to collisional stopping. The color-filled areas represent uncertainties in the model. The solid-density Ti target is assumed.

Published under license by AIP Publishing

An important point to be made is that the resistive heating is dominating compared to the collisional heating. This is demonstrated in Fig. 5(a) by showing the calculated temperature with the resistive heating omitted. This will also be seen below in connection with the beam stopping.

B. Beam stopping power

The present work allows us to investigate the beam stopping power and, in particular, to elucidate the resistive stopping due to the return current and compare it with the direct collisional contribution to the stopping power. The former contribution is obtained by assuming that the energy involved in heating of the target due to the return current is provided by the beam.

In Fig. 5(b), we present a ratio of the resistive to the collisional stopping, which within our model (see Sec. III B) is

$$P_{\mathrm{res}}/P_{\mathrm{col}} = \eta j e/S. \tag{6}$$

The dominance of the resistive stopping, which increases with time and beam intensity, is clearly seen. We note that the resistive stopping does not scale with the current density squared since the resistivity varies with the target temperature, decreasing strongly toward the Spitzer regime.

As an example, we calculate the energy loss of a 1-MeV beam traversing a 25-μm-thick foil target. The results are presented in Table III for the two different current densities inferred assuming the regular and enhanced dE/dx in the calibration procedure (see Table I). It is observed that the resistive stopping dominates. This is in agreement with a very recent study by Chawla *et al.*[30] who found that for Al and Cu, the resistive stopping is about 4–5 times larger than the collisional one.

V. CONCLUSIONS

The objective of this study is to theoretically obtain results, which can be compared with the experimental data[13] on the target heating in ultra-intense femtosecond laser–target interactions. This was accomplished by means of a straightforward physical modeling, essentially with no free parameters. Importantly, the fast electron current was inferred from absolutely calibrated experimental data, not relying upon assumptions about the energy conversion.

The basic physical entities involved in the calculations are the specific heat of the electronic component of the target material and its resistivity. The former was calculated by means of the average-atom model. The latter was obtained using measured resistivity data in a similar type of experiment and augmented by sound scaling considerations. Although not perfect, the accuracy of thus derived data is sufficient for our purposes. Note that for some species, in particular, aluminum, accurate measurements or *ab initio* calculations exist. See, for example, recent studies of Cytter *et al.*[53] and Driver, Soubiran, and Militzer[54] for calculations of the heat capacity and Sperling *et al.*[55] and Witte *et al.*[56] for measurements and calculations of resistivity. However, to the best of our knowledge, neither theoretical nor experimental data have been published for titanium.

The modeling involved a few simplifying assumptions, some of them related to the time-integrated nature of the experimental data available. Nevertheless, despite a certain ambiguity in interpretation of the experimental time-integrated temperature and uncertainties in the calculations, we find the agreement between experiment and theory to be good. It is also noteworthy to point out the dominance of the return-current heating compared to the direct one for the conditions of this experiment, as well as the dramatic increase in beam stopping power due to this process.

We believe that the approach here described can be applied to modeling and analysis of other experiments of a similar kind.

TABLE III. The resistive ΔE_{res} and total ΔE_{tot} energy losses of a 1-MeV electron traversing a 25-μm Ti target. The 15-keV difference is due to the direct-heating contribution.

j (A/cm^2)	ΔE_{res} (keV)	ΔE_{tot} (keV)
1.8×10^{11}	53	68
2.3×10^{11}	88	103

ACKNOWLEDGMENTS

This work was supported in part by the Minerva Foundation (Germany).

DATA AVAILABILITY

The data that support the findings of this study are available from the corresponding author upon reasonable request.

REFERENCES

[1] J. R. Davies, A. R. Bell, M. G. Haines, and S. M. Guérin, "Short-pulse high-intensity laser-generated fast electron transport into thick solid targets," Phys. Rev. E **56**, 7193–7203 (1997).
[2] A. P. L. Robinson, D. J. Strozzi, J. R. Davies, L. Gremillet, J. J. Honrubia, T. Johzaki, R. J. Kingham, M. Sherlock, and A. A. Solodov, "Theory of fast electron transport for fast ignition," Nucl. Fusion **54**, 054003 (2014).
[3] A. Macchi, M. Borghesi, and M. Passoni, "Ion acceleration by superintense laser-plasma interaction," Rev. Mod. Phys. **85**, 751–793 (2013).
[4] D. Riley, "Generation and characterisation of warm dense matter with intense lasers," Plasma Phys. Controlled Fusion **60**, 014033 (2017).
[5] M. S. Murillo, "Strongly coupled plasma physics and high energy-density matter," Phys. Plasmas **11**, 2964 (2004).
[6] E. Martinolli, M. Koenig, S. D. Baton, J. J. Santos, F. Amiranoff, D. Batani, E. Perelli-Cippo, F. Scianitti, L. Gremillet, R. Melizzi, A. Decoster, C. Rousseaux, T. A. Hall, M. H. Key, R. Snavely, A. J. MacKinnon, R. R. Freeman, J. A. King, R. Stephens, D. Neely, and R. J. Clarke, "Fast-electron transport and heating of solid targets in high-intensity laser interactions measured by K alpha fluorescence," Phys. Rev. E **73**, 046402–046405 (2006).
[7] J. J. Santos, A. Debayle, P. Nicolaï, V. Tikhonchuk, M. Manclossi, D. Batani, A. Guemnie-Tafo, J. Faure, V. Malka, and J. J. Honrubia, "Fast-electron transport and induced heating in aluminum foils," Phys. Plasmas **14**, 103107 (2007).
[8] J. J. Santos, D. Batani, S. D. Baton, F. N. Beg, T. Ceccotti, A. Debayle, F. Dorchies, J.-L. Feugeas, C. Fourment, L. Gremillet, J. J. Honrubia, S. Hulin, A. Morace, P. Nicolaï, F. Pérez, H. Sawada, H.-P. Schlenvoigt, V. T. Tikhonchuk, X. Vaisseau, B. Vauzour, and M. Wei, "Supra-thermal electron beam stopping power and guiding in dense plasmas," J. Plasma Phys. **79**, 429–435 (2013).
[9] J. J. Honrubia, A. Antonicci, and D. Moreno, "Hybrid simulations of fast electron transport in conducting media," Laser Part. Beams **22**, 129–135 (2004).
[10] M. Passoni, V. T. Tikhonchuk, M. Lontano, and V. Y. Bychenkov, "Charge separation effects in solid targets and ion acceleration with a two-temperature electron distribution," Phys. Rev. E **69**, 026411 (2004).
[11] F. Perez, L. Gremillet, M. Koenig, S. D. Baton, P. Audebert, M. Chahid, C. Rousseaux, M. Drouin, E. Lefebvre, T. Vinci, J. Rassuchine, T. Cowan, S. A. Gaillard, K. A. Flippo, and R. Shepherd, "Enhanced isochoric heating from fast electrons produced by high-contrast, relativistic-intensity laser pulses," Phys. Rev. Lett. **104**, 085001 (2010).

Published under license by AIP Publishing

[12]A. Soloviev, K. Burdonov, S. N. Chen, A. Eremeev, A. Korzhimanov, G. V. Pokrovskiy, T. A. Pikuz, G. Revet, A. Sladkov, V. Ginzburg, E. Khazanov, A. Kuzmin, R. Osmanov, I. Shaikin, A. Shaykin, I. Yakovlev, S. Pikuz, M. Starodubtsev, and J. Fuchs, "Experimental evidence for short-pulse laser heating of solid-density target to high bulk temperatures," Sci. Rep. **7**, 12144 (2017).
[13]U. Zastrau, P. Audebert, V. Bernshtam, E. Brambrink, T. Kämpfer, E. Kroupp, R. Loetzsch, Y. Maron, Y. Ralchenko, H. Reinholz, G. Röpke, A. Sengebusch, E. Stambulchik, I. Uschmann, L. Weingarten, and E. Förster, "Temperature and $K\alpha$-yield radial distributions in laser-produced solid-density plasmas imaged with ultra-high-resolution x-ray spectroscopy," Phys. Rev. E **81**, 026406 (2010).
[14]U. Zastrau, A. Sengebusch, P. Audebert, E. Brambrink, R. R. Faüstlin, T. Kämpfer, E. Kroupp, R. Loetzsch, Y. Maron, H. Reinholz, G. Röpke, E. Stambulchik, I. Uschmann, and E. Förster, "High-resolution radial Kα spectra obtained from a multi-keV electron distribution in solid density titanium foils generated by relativistic laser–matter interaction," High Energy Density Phys. **7**, 47–53 (2011).
[15]E. Nardi, Z. Zinamon, and Y. Maron, "Energy content of target and electron flow in femtosecond laser target interactions," Laser Part. Beams **33**, 245–256 (2015).
[16]E. Nardi, Z. Zinamon, E. Stambulchik, E. Kroupp, and Y. Maron, "Detailed analysis of thin foil Kα experimental data in ultra-intense laser–target interactions: Electron refluxing, TNSA model, and probing electric field outside the foil," (unpublished).
[17]V. T. Tikhonchuk, "Interaction of a beam of fast electrons with solids," Phys. Plasmas **9**, 1416–1421 (2002).
[18]B. Vauzour, J. J. Santos, A. Debayle, S. Hulin, H.-P. Schlenvoigt, X. Vaisseau, D. Batani, S. D. Baton, J. J. Honrubia, P. Nicolaï, F. N. Beg, R. Benocci, S. Chawla, M. Coury, F. Dorchies, C. Fourment, E. d'Humières, L. C. Jarrot, P. McKenna, Y. J. Rhee, V. T. Tikhonchuk, L. Volpe, and V. Yahia, "Relativistic high-current electron-beam stopping-power characterization in solids and plasmas: Collisional versus resistive effects," Phys. Rev. Lett. **109**, 255002 (2012).
[19]L. Volpe, D. Batani, A. Morace, and J. J. Santos, "Collisional and collective effects in two dimensional model for fast-electron transport in refluxing regime," Phys. Plasmas **20**, 013104 (2013).
[20]E. Stambulchik, V. Bernshtam, L. Weingarten, E. Kroupp, D. Fisher, Y. Maron, U. Zastrau, I. Uschmann, F. Zamponi, E. Förster, A. Sengebusch, H. Reinholz, G. Röpke, and Yu. Ralchenko, "Progress in line-shape modeling of K-shell transitions in warm dense titanium plasmas," J. Phys. A: Math. Theor. **42**, 214056 (2009).
[21]K. Eidmann, U. Andiel, F. Pisani, P. Hakel, R. C. Mancini, G. C. Junkel-Vives, J. Abdallah, and K. Witte, "K-shell spectra from hot dense aluminum layers buried in carbon and heated by ultrashort laser pulses," J. Quant. Spectrosc. Radiat. Transfer **81**, 133–146 (2003).
[22]T. Kluge, M. Bussmann, U. Schramm, and T. E. Cowan, "Simple scaling equations for electron spectra, currents, and bulk heating in ultra-intense short-pulse laser-solid interaction," Phys. Plasmas **25**, 073106 (2018).
[23]J. R. Davies, "Electric and magnetic field generation and target heating by laser-generated fast electrons," Phys. Rev. E **68**, 056404 (2003).
[24]J. R. Davies, J. S. Green, and P. A. Norreys, "Electron beam hollowing in laser–solid interactions," Plasma Phys. Controlled Fusion **48**, 1181–1199 (2006).
[25]R. J. Garland, M. Borghesi, and A. P. L. Robinson, "Analysis of the fast electron scaling theory for the heating of a solid target," Phys. Plasmas **23**, 083116 (2016).
[26]J. S. Green, V. M. Ovchinnikov, R. G. Evans, K. U. Akli, H. Azechi, F. N. Beg, C. Bellei, R. R. Freeman, H. Habara, R. Heathcote, M. H. Key, J. A. King, K. L. Lancaster, N. C. Lopes, T. Ma, A. J. MacKinnon, K. Markey, A. McPhee, Z. Najmudin, P. Nilson, R. Onofrei, R. Stephens, K. Takeda, K. A. Tanaka, W. Theobald, T. Tanimoto, J. Waugh, L. Van Woerkom, N. C. Woolsey, M. Zepf, J. R. Davies, and P. A. Norreys, "Effect of laser intensity on fast-electron-beam divergence in solid-density plasmas," Phys. Rev. Lett. **100**, 015003 (2008).
[27]M. Coury, D. C. Carroll, A. P. L. Robinson, X. H. Yuan, C. M. Brenner, M. Burza, R. J. Gray, K. L. Lancaster, Y. T. Li, X. X. Lin, D. A. MacLellan, H. Powell, M. N. Quinn, O. Tresca, C.-G. Wahlström, D. Neely, and P. McKenna, "Injection and transport properties of fast electrons in ultraintense laser-solid interactions," Phys. Plasmas **20**, 043104 (2013).
[28]T. S. Daykin, H. Sawada, Y. Sentoku, F. N. Beg, H. Chen, H. S. McLean, A. J. Link, P. K. Patel, and Y. Ping, "Characterization of fast electron divergence and energy spectrum from modeling of angularly resolved bremsstrahlung measurements," Phys. Plasmas **25**, 123103 (2018).
[29]A. R. Bell and R. J. Kingham, "Resistive collimation of electron beams in laser-produced plasmas," Phys. Rev. Lett. **91**, 035003 (2003).
[30]S. Chawla, M. Bailly-Grandvaux, H. S. McLean, P. K. Patel, M. S. Wei, and F. N. Beg, "Effect of target material on relativistic electron beam transport," Phys. Plasmas **26**, 033111 (2019).
[31]M. E. Glinsky, "Regimes of suprathermal electron transport," Phys. Plasmas **2**, 2796–2806 (1995).
[32]A. R. Bell, J. R. Davies, S. Guerin, and H. Ruhl, "Fast-electron transport in high-intensity short-pulse laser-solid experiments," Plasma Phys. Controlled Fusion **39**, 653–659 (1997).
[33]E. Lefebvre, L. Gremillet, A. Lévy, R. Nuter, P. Antici, M. Carrié, T. Ceccotti, M. Drouin, J. Fuchs, V. Malka, and D. Neely, "Proton acceleration by moderately relativistic laser pulses interacting with solid density targets," New J. Phys. **12**, 045017 (2010).
[34]H. A. Bethe, "Molière's theory of multiple scattering," Phys. Rev. **89**, 1256–1266 (1953).
[35]E. Nardi and Z. Zinamon, "Energy deposition by relativistic electrons in high-temperature targets," Phys. Rev. A **18**, 1246–1249 (1978).
[36]B. L. Henke, E. M. Gullikson, and J. C. Davis, "X-ray interactions: Photoabsorption, scattering, transmission, and reflection at E = 50–30 000 eV, Z = 1–92," At. Data Nucl. Data Tables **54**, 181–342 (1993).
[37]X. Llovet, C. J. Powell, F. Salvat, and A. Jablonski, "Cross sections for inner-shell ionization by electron impact," J. Phys. Chem. Ref. Data **43**, 013102 (2014).
[38]M. O. Krause, "Atomic radiative and radiationless yields for k and l shells," J. Phys. Chem. Ref. Data **8**, 307–327 (1979).
[39]S. Eliezer, N. Eliaz, E. Grossman, D. Fisher, I. Gouzman, Z. Henis, S. Pecker, Y. Horovitz, M. Fraenkel, S. Maman, and Y. Lereah, "Synthesis of nanoparticles with femtosecond laser pulses," Phys. Rev. B **69**, 144119 (2004).
[40]M. J. Berger and S. M. Seltzer, "Tables of energy losses and ranges of electrons and positrons," in *Studies in Penetration of Charged Particles in Matter* (National Academies, Washington, DC, 1964), p. 205–268; M. J. Berger, M. Inokuti, H. H. Anderson, H. Bichsel, J. A. Dennis, D. Powers, S. M. Seltzer, and J. E. Turner, *ICRU Report 37: Stopping Powers and Ranges for Electrons and Positrons* (Oxford Academic, 1984), Vol. os19.
[41]D. A. Liberman, "Self-consistent field model for condensed matter," Phys. Rev. B **20**, 4981–4989 (1979).
[42]Z. Lin, L. V. Zhigilei, and V. Celli, "Electron–phonon coupling and electron heat capacity of metals under conditions of strong electron–phonon non-equilibrium," Phys. Rev. B **77**, 075133 (2008).
[43]A. S. Sandhu, A. K. Dharmadhikari, and G. R. Kumar, "Time resolved evolution of structural, electrical, and thermal properties of copper irradiated by an intense ultrashort laser pulse," J. Appl. Phys. **97**, 023526 (2004).
[44]N. F. Mott, "The electrical resistivity of liquid transition metals," Philos. Mag. **26**, 1249–1261 (1972).
[45]H. M. Milchberg, R. R. Freeman, S. C. Davey, and R. M. More, "Resistivity of a simple metal from room temperature to 10^6 K," Phys. Rev. Lett. **61**, 2364–2367 (1988).
[46]K. Eidmann, J. Meyer-ter Vehn, T. Schlegel, and S. Hüller, "Hydrodynamic simulation of subpicosecond laser interaction with solid-density matter," Phys. Rev. E **62**, 1202–1214 (2000).
[47]G. Faussurier and C. Blancard, "Resistivity saturation in warm dense matter," Phys. Rev. E **91**, 013105 (2015).
[48]N. Wetta and J.-C. Pain, "Consistent approach for electrical resistivity within Ziman's theory from solid state to hot dense plasma: Application to aluminum," Phys. Rev. E **102**, 053209 (2020).
[49]N. W. Ashcroft and N. D. Mermin, *Solid State Physics* (Saunders College, Philadelphia, PA, 1976).
[50]B. P. Panda, "Electronic structure and equilibrium properties of hcp titanium and zirconium," Pramana J. Phys. **79**, 327–335 (2012).
[51]D. A. MacLellan, D. C. Carroll, R. J. Gray, N. Booth, M. Burza, M. P. Desjarlais, F. Du, B. Gonzalez-Izquierdo, D. Neely, H. W. Powell, A. P. L. Robinson, D. R. Rusby, G. G. Scott, X. H. Yuan, C.-G. Wahlström, and P. McKenna, "Annular fast electron transport in silicon arising from low-temperature resistivity," Phys. Rev. Lett. **111**, 095001 (2013).

Published under license by AIP Publishing

[52]Y. T. Lee and R. M. More, "An electron conductivity model for dense plasmas," Phys. Fluids **27**, 1273–1286 (1984).
[53]Y. Cytter, E. Rabani, D. Neuhauser, and R. Baer, "Stochastic density functional theory at finite temperatures," Phys. Rev. B **97**, 115207 (2018).
[54]K. P. Driver, F. Soubiran, and B. Militzer, "Path integral Monte Carlo simulations of warm dense aluminum," Phys. Rev. E **97**, 063207 (2018).
[55]P. Sperling, E. J. Gamboa, H. J. Lee, H. K. Chung, E. Galtier, Y. Omarbakiyeva, H. Reinholz, G. Röpke, U. Zastrau, J. Hastings, L. B. Fletcher, and S. H. Glenzer, "Free-electron X-ray laser measurements of collisional-damped plasmons in isochorically heated warm dense matter," Phys. Rev. Lett. **115**, 115001 (2015).
[56]B. B. L. Witte, L. B. Fletcher, E. Galtier, E. Gamboa, H. J. Lee, U. Zastrau, R. Redmer, S. H. Glenzer, and P. Sperling, "Warm dense matter demonstrating non-Drude conductivity from observations of nonlinear plasmon damping," Phys. Rev. Lett. **118**, 225001 (2017); B. B. L. Witte, P. Sperling, M. French, V. Recoules, S. H. Glenzer, and R. Redmer, "Observations of non-linear plasmon damping in dense plasmas," Phys. Plasmas **25**, 056901 (2018).

Published under license by AIP Publishing